Archives of Hydro-Engineering and Environmental Mechanics
Vol. 58 (2011), No. 1–4, pp. 65–86
DOI: 10.2478/v10203-011-0004-7

Spatially Averaged Log-Law for Flows over Rough Bed in Zero- and Non-Zero-Pressure Gradient Boundary Layers

Włodzimierz Czernuszenko

Institute of Geophysics Polish Academy of Sciences, 01-452 Warsaw, Ks. Janusza 64, Poland,
e-mail: wczer@igf.edu.pl

(Received June 03, 2011; revised September 12, 2011)

Abstract

Theoretical bases for building a logarithmic law for non-uniform flows over a large relative roughness are presented. In order to define the equivalent velocity distribution and to smooth out 3D flow irregularities, a special spatial averaging operation is defined. Basic equations are spatially averaged and double-averaged momentum equations for primary component velocity are derived for uniform flow over a gravel bed as well as for non-uniform flows. A new hypothesis is proposed, and some assumptions are introduced to solve these momentum equations. This results in a new version of the logarithmic velocity distribution (log law). To define this distribution, a full reconstruction of Nikuradse's graph for flows over an irregular gravel riverbed is considered. It is based on very precise measurements of velocity and other hydraulic parameters. In the case of non-uniform flows, the logarithmic velocity profile appears also in accelerating flows in a gravel bed channel, but the friction velocity should be re-defined according to Eq. (24). The same applies to decelerating flow with a positive pressure gradient, but only if the gravitational force exceeds the pressure gradient. For accelerating flows, the additive constant B_P depends on the pressure gradient, and its values grow with a growing pressure gradient.

Key words: open channel, log-law, non-uniform flow, rough flow, accelerating flows, decelerating flows

Notations

$<>$	–	double-averaged quantity,
B	–	universal (additive) constant in the log law,
Bp	–	additive constant in the log law for flow in a non-zero-pressure gradient,
D_{50}	–	median diameter of gravel,
D_s	–	grain diameter,
h	–	water depth,
k	–	absolute size of roughness elements,

k_{ef} – height of the average roughness interfering with the flow,
P – time-average pressure,
S_0 – slope of the channel bed,
S_f – slope of the energy gradient line,
U, V, W or u, v, w – corresponding velocity components,
U_i – i-th components of the time-average velocity,
u_i – i-th components of the turbulent velocity,

$$U_i(x, y, z, t) = U(x, y, z) + u_i(x, y, z, t),$$

x – horizontal (longitudinal) coordinate,
y – vertical coordinate,
y_0 – location of the velocity origin (the effective velocity origin),
y_t – location of the velocity origin below the top of the roughness element,
z – lateral (horizontal) coordinate,
κ – von Karman's constant,
κ_e – von Karman's constant related to the mixing length l_e,
ν – kinematic viscosity,
ρ – mass density of the fluid,
ρ_s – mass density of the sediment,
τ_f – form-induced stresses or form stresses,
τ_t – mean Reynolds stresses,
$\Phi(y)$ – roughness geometry function.

1. Introduction

The vertical profile of the mean velocity in an open-channel flow is of great interest to engineers, particularly for both uniform and non-uniform flows over gravel beds. The boundary of a channel is usually rough, and roughness elements interfere with the flow. These interferences produce a complicated flow pattern even in the region away from the boundary, especially in the case of non-uniform flows. This effect is most pronounced when the size of roughness elements is relatively large, for example, in the case of a gravel or pebble bed. Nikuradse's concept of a logarithmic velocity profile with the absolute size of roughness elements k and the universal constant B, can be used only for sand roughness (Yalin 1977). When the relative spacing, size and shape of roughness elements are particularly important, Nikuradse's concept becomes problematic. Nevertheless, Nikuradse's sand grain roughness has become a standard method of describing the roughness of the boundary in both pipes and open-channel flows.

Two types of large relative roughness are distinguished. In the first case, some roughness elements, such as boulders, are spread on the river bed and might protrude into the water surface. In the second, the bed is composed of coarse but relatively uniform materials. The second case is similar to sand roughness, the difference being that the relative roughness is much greater, and the whole flow may directly the influence of bed materials (Tu 1991). The object of the present investigation is the second case, i.e., riverbeds covered with coarse but relatively uniform materials. In both cases, however, turbulent flow characteristics are strongly influenced by the heterogeneity of the bed topography. Therefore the near-bed time-averaged flow is spatially heterogeneous and the double average method (DAM) can produce meaningful estimation for two-dimensional flow (see Nikora et al 2001). The method consists of averaging Navier-Stokes equations in time and space over a surface area parallel to the flow direction.

On the basis of laboratory measurements of velocity over several roughness heights (diameter of river gravel and pebbles) from $D = 0.5$ mm to 40 mm, Kamphuis (1974) concluded that the diameter was a poor roughness criterion. The logarithmic velocity distribution is valid when the average size of roughness elements ranges from $k = 1.5D$ to $k = 2.5D$, and the universal constant is 8.5 (this constant is denoted by B, see Eq. (15)). The actual point where the velocity is zero (effective velocity origin) has been found $0.3D$ below the crest of roughness elements.

When the roughness size is large in relation to the flow depth, it is important to locate the theoretical (virtual) bottom, where $y = 0$. Bayazit (1976), in his experiments with hemispheres of diameter $D = 23$ mm, found that the theoretical bed would have to lie at a distance of $0.35D$ below the tops of the hemispheres in order that the velocity distribution agrees with the logarithmic law. He showed that the usual log law remains valid for velocity distribution as long as the flow depth is greater than the roughness height. The equivalent sand roughness in this case is $2.5D$, and the universal constant $B = 8.5$.

Kirkgoz (1989) investigates the velocity distribution in rough boundary flows with roughness elements of different sizes, namely $k = 1$ mm, 4 mm, 8 mm and 12 mm. The experimental values of the position of the reference level, where the mean velocity is zero, lie between 0.25 mm and 0.75 mm below the tops of roughness elements. Finally, he concludes that the size of roughness elements is reflected in the values of the friction velocity, and the friction velocity U_* increases with the increasing roughness size.

It is common to distinguish two regions for the velocity profile: the inner or wall region, and the outer or core region. The velocity distribution in the inner region follows a log law, and in the wake region are some deviations from the log law. To reduce these deviations, some authors suggest that the additive constant should increase with the Reynolds number in this region (Guo et al 2005). However, in practice the log law is frequently applied to the whole outer region, i.e., from the bottom to the surface.

Also, it is possible to distinguish an interfacial sublayer, which is the vertical distance from the virtual bed ($y = 0$) to the top of the maximum elevation of the gravel bed. Nikora et al (2001) studied flow over an array of spherical elements as the bed roughness and showed that the double-averaged streamwise velocity distribution is approximately linear within the interfacial sublayer.

The case of non-uniform open-channel shear flows, namely accelerating flows, which occur when the flow velocity increases along its path, thus creating a boundary layer with a negative pressure gradient, will be analyzed on the basis of data from Afzalimehr and Anctil (2000). Decelerating flows with a positive pressure force will only be analyses theoretically because of the lack of data.

The main aims of the work are (1) to develop basic equations for vertical velocity profiles for both uniform and non-uniform flows over rough beds, i.e., a log law for the flow with a non-zero-pressure gradient; (2) to re-construct Nikuradse's graph for uniform flows over roughness elements (not for sand-bed roughness); and (3) to show that the constant B is not universal and depends on the roughness geometry and on the pressure gradient in the case of non-uniform flows.

2. Basic Hydrodynamic Equations

Three-dimensional steady turbulent flow in an open channel is governed by the Reynolds-averaged Navier-Stokes equations. The continuity and momentum equations for incompressible turbulent flows may be written in the Cartesian tensor notation in the following forms:

– continuity equation

$$\frac{\partial U_i}{\partial x_i} = 0, \tag{1}$$

– momentum equations

$$U_j \frac{\partial U_i}{\partial x_j} = -\frac{1}{\rho}\frac{\partial P}{\partial x_i} + F_i - \frac{\partial}{\partial x_j}\left(\overline{u_i u_j} - \nu \frac{\partial U_i}{\partial x_j}\right), \tag{2}$$

where U_i and u_i are the i-th components of the time-average velocity and turbulent velocity, respectively, so that $U_i\ (x, y, z, t) = U(x, y, z) + u_i(x, y, z, t)$; P is time-average pressure, ρ is density, ν is kinematic viscosity, g is the acceleration of gravity, and $\mathbf{F} = (g \sin\theta, g \cos\theta, 0)$. The following notation will be used in this paper: x, y, z for horizontal (longitudinal), vertical and lateral coordinates, respectively, and U, V, W or u, v, w for the corresponding velocity components.

These equations are not suitable for engineering problems because of a highly 3D structure of the mean flow, especially for gravel bed materials. In this case, the flow, at least in the very close neighborhood of an irregular rough boundary, is strongly heterogeneous spatially. By applying the procedure of spatial averaging to the above equations, they can be made much simpler and easy to integrate, Nikora et al (2004).

2.1. The Phase Averaging Theorem: Flows in the Interfacial Layer

The interfacial layer occupies the flow region between roughness crests and troughs. To establish an equation for flow in this layer, a special averaging operation is introduced (for details see Nikora et al 2007). The averaging area (A) is composed of the area of the continuous phase, i.e. fluid (A_f), and the areas occupied by the solid phase, i.e. roughness elements (A_s). The area has to be large enough so that a small increase in the area would not affect the value of the average. Let K be some property of the continuous phase per unit volume. The phase average, sometimes described as the intrinsic average of K (see Slattery 1999), is the average over the area of the continuous phase and is defined as

$$\langle K \rangle = \frac{1}{A_f} \int_{A_f} K dA = \frac{1}{\phi\, A} \int_{A_f} K dA, \tag{3}$$

where $\phi(y)$ is the roughness geometry function and is defined as the ratio of $A_f(y)/A$. The domain of the integral in Eq. (3) is the rectangular area parallel to the plane y = const (assumed as parallel to the mean bed) centered at the point (x, z). The area of the domain should be wide enough in comparison with the characteristic wavelength of the lateral disturbances of the velocity distribution and long enough in comparison with the characteristic wavelength of longitudinal disturbances.

The area-averaging theorem for rigid roughness or frozen roughness elements can be defined by analogy with the volume-averaging theorem by the formula (see Slattery 1999)

$$\left\langle \frac{\partial K}{\partial x_i} \right\rangle = \frac{1}{\phi} \frac{\partial \phi \langle K \rangle}{\partial x_i} - \frac{1}{A_f} \int_{L_{int}} K n_i dL, \tag{4}$$

where n_i is a unit normal vector directed away from the roughness elements and L_{int} is the interface between the roughness elements and the fluid.

According to Eq. (4), the surface average of the gradient is the gradient of the surface average plus an additional term which involves the integral of K over the interface between the roughness elements and the fluid. The property K can be a scalar, vector or second-order tensor. Now, the time-averaged equations are to be subjected to spatial area averaging, but first the ensemble average variable (velocity and pressure) is split into a double-averaged variable and a deviation from this average (indicated by the wave overbar in Eq. (5)) according to

$$\begin{aligned} U(x,y,z) &= \langle U(y) \rangle + \widetilde{u}\,(x,y,z) \quad \text{for all } (x,z) \in A, \quad \langle \widetilde{u} \rangle = 0, \\ P(x,y,z) &= \langle P(y) \rangle + \widetilde{p}(x,y,z) \qquad\qquad\qquad\quad \langle \widetilde{p} \rangle = 0, \end{aligned} \tag{5}$$

where the wave overbar denotes a disturbance in flow variables, i.e., the difference between the double-averaged and time-averaged values.

One notes that the double-averaged variables are the same at all points belonging to the area of averaging. It is convenient to relate these variables with the location of the center of gravity of the area of averaging A. If appropriate sizes of the averaging area are chosen, the averaging variables are a function of the vertical coordinate only. Applying Eqs. (4)–(5) to average the momentum and continuity equations, one can obtain the so-called double-averaged (in time and space) equations for the conservation of momentum (see Nikora et al 2007),

$$\left\langle U_j \right\rangle \frac{\partial \langle U_i \rangle}{\partial x_j} = g_i - \frac{1}{\phi\rho}\frac{\partial \phi \langle P \rangle}{\partial x_i} - \frac{1}{\phi}\frac{\partial \phi \left\langle \overline{u_i u_j} \right\rangle}{\partial x_j} - \frac{1}{\phi}\frac{\partial \phi \left\langle \widetilde{u_i}\widetilde{u_j} \right\rangle}{\partial x_j} + \\ + \frac{1}{\phi}\frac{\partial}{\partial x_j}\phi \left\langle \nu \frac{\partial U_i}{\partial x_j} \right\rangle + \frac{1}{A_f \rho}\int\limits_{Lint} \widetilde{p} n_i dL - \frac{1}{A_f}\int\limits_{Lint} \left(\nu \frac{\partial U_i}{\partial x_j} \right) dL \tag{6}$$

and the double-averaged continuity equation

$$\frac{\partial \phi \langle U_i \rangle}{\partial x_i} = 0. \tag{7}$$

Please note that the deviations of the velocities in time and space are not correlated to each other.

Some information about the double-averaging methodology (DAM) can be obtained from measurements only. Aberle et al (2008) carried out a laboratory experiment in a 0.90 m wide and 0.60 m high tilting flume, where coarse sediment mixtures in a range of 0.63–64 mm were used as movable bed materials. The 3D bed topography of the stable armor layer was estimated from surface scans of the bed with a laser displacement meter within a 2.4 m long and 0.36 m wide test section. These data were used to determine the roughness geometry function. Values of this function vary almost linearly from 0 to 1 along the distance from the minimum to maximum bed elevation, except close to the top of the roughness elements, where they grow more quickly from 0.8 to 1 (see Aberle 2007 for details).

3. Uniform Flows Above the Crests of Roughness Elements

Equations (6) and (7) are valid for flow regions both above and below roughness tops. Note that for the region above roughness tops all terms containing derivatives of phi (Φ) and two integrals in Eq. (6) disappear, as does Φ in other terms, so Eq. (6) takes the form

$$\left\langle U_j \right\rangle \frac{\partial \langle U_i \rangle}{\partial x_j} = g_i - \frac{1}{\rho}\frac{\partial \langle P \rangle}{\partial x_i} - \frac{\partial \left\langle \overline{u_i u_j} \right\rangle}{\partial x_j} - \frac{\partial \left\langle \widetilde{u_i}\widetilde{u_j} \right\rangle}{\partial x_j} + \frac{\partial}{\partial x_j}\left\langle \nu \frac{\partial U_i}{\partial x_j} \right\rangle. \tag{8}$$

It is very natural to assume that for a wide open-channel flow (more exactly, for a large aspect ratio) all terms in the lateral, z-momentum equation are zero, and

for uniform flow the convective inertia term is negligibly small compared with the others. Also, it is easy to show that the y-momentum equation gives the vertical pressure distribution very close to the hydrostatic one, and its gradient is equal to zero, but the x-momentum equation is simplified to

$$\frac{\partial}{\partial y}\left(-\left\langle\overline{u'\,v'}\right\rangle-\langle\widetilde{u}\,\widetilde{v}\rangle+\nu\frac{\partial\langle U\rangle}{\partial y}\right)=-gS_0, \tag{9}$$

where $S_0 = -\tan\theta \sim -\sin\alpha$ is the slope of the bed.

After the integration of Eq. (9) across the boundary layer (above roughness tops), one can receive a formula for the distribution of the total shear stresses in the form

$$\frac{\tau_{total}(y)}{\rho}=\left(-\left\langle\overline{u'\,v'}\right\rangle-\langle\widetilde{u}\,\widetilde{v}\rangle+\nu\frac{\partial\langle U\rangle}{\partial y}\right)=ghS_0\left(1-\frac{y}{h}\right). \tag{10}$$

Hence, the total shear stresses vary linearly with y. They become equal to zero at the free surface (where $y = h$), and it is assumed that they reach their maximum value at the roughness height but not at the virtual bed (where $y = 0$), because Eq. (9) is not valid at $y = 0$. Aberle et al (2008) showed that the peaks of form-induced stresses are located just below roughness tops (see Figure 1).

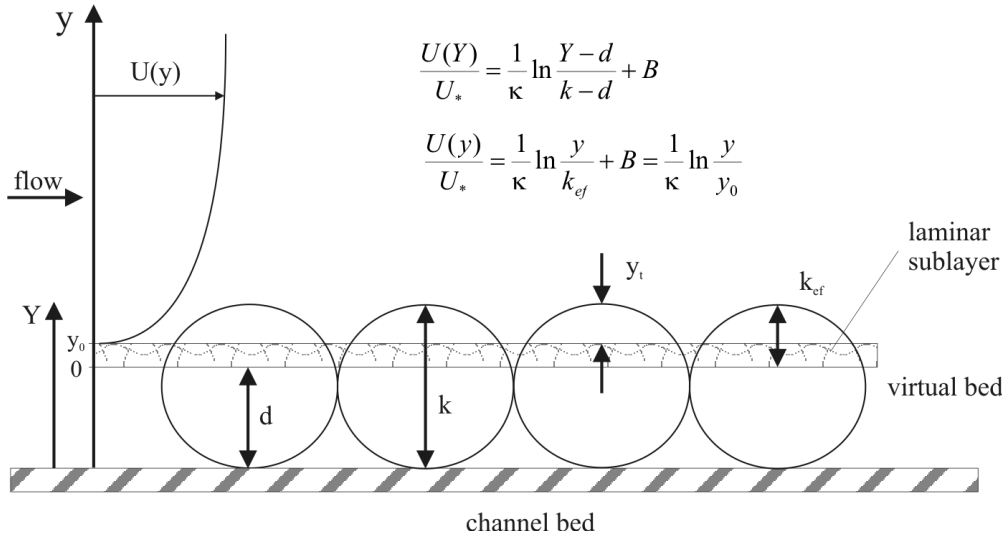

Fig. 1. Basic definitions of the log law for flows over spherical roughness elements: the absolute size of roughness elements k is the diameter of spherical roughness elements, d is the zero-plane displacement, k_{ef} is the height of the roughness interfering with the flow (for details see McLean et al 2002)

The total shear stresses can be expressed as a sum of three components: the mean Reynolds (τ_t) stresses; new stresses (τ_f), called "form-induced stresses" or simply

"form stresses" (see Gimenez-Curto and Corniero Lera 1996); and the mean viscous (τ_v) stresses. It is therefore assumed that the bed shear stress has three components, τ_{ot}, τ_{of} and τ_{ov} , and it appears somewhere below the roughness height. Starting at this level, viscous shear stresses become negligibly small compared with the other two stresses. Viscous stresses are essential only in the viscous sublayer, in which the other two stresses are negligibly small compared with viscous stress. The thickness of the viscous sub-layer is very difficult to estimate, but it is approximately less than 15% of k_s for a rough sand bed (Yalin 1977). This means that the shear stress due to the molecular viscosity μ (viscous shear stress) for the viscous sub-layer is given by

$$\tau_l(y) = \mu \frac{d\langle U\rangle}{dy}. \tag{11}$$

Outside the viscous sublayer (in a fully turbulent flow), the viscous stress in Eq. (10) is negligibly small in comparison with the others. Thus, the total shear stresses (in the wall region, $y < 0.2$ depth) can be modeled by Prandtl's mixing length hypothesis (MLH) as follows:

$$\tau_{total} = \rho\, l_e^2 \left(\frac{\partial\langle U\rangle}{\partial y}\right)^2, \tag{12}$$

where l_e is a length scale defined in the framework of double average methodology (DAM) by analogy with Prandtl's mixing length. It is measured from the bed origin.

It is reasonable to assume (by analogy with the behavior of the log law) that a double-averaged velocity profile can be obtained from Eq. (12) with a constant total stress. This equation with the assumption that $l_e = \kappa_e y$ (κ_e is von Karman's constant related to the mixing length l_e) can be easily integrated in the "turbulent core" outside the viscous sub-layer, i.e., in the interval $[y_k, y]$

$$\frac{\langle U(y)\rangle}{U_*} = \frac{1}{\kappa_e} \ln\frac{y}{y_k} + \frac{\langle U_k\rangle}{U_*}, \tag{13}$$

where U_k is the value of U at the top of averaged roughness elements, i.e. at $y_k = k_{ef}$, where k_{ef} is the height of the averaged roughness interfering with the flow; it will be assumed that $\kappa_e = \kappa = 0.4$ universal von Karman's constant, which is independent of the nature of the wall, whether smooth or rough. The shear velocity U_* is the most fundamental scale, and there are several methods to estimate this scale. For the zero pressure-gradient model, we usually use the formula $U* = (ghS_0)^{0.5}$, where S_0 is the bed slope. It is also possible to use Clauser's method (1956), which relies on the validity of the logarithmic law for the inner (wall) region of the boundary layer ($y/h < 0.2$).

The above solution is true only for small distances from the wall, i.e., in the inner layer, where the mixing length varies linearly with the distance and the shear

stress is a constant. The second term of Eq. (13), called the roughness function, is a non-dimensional quantity related to flow over rough walls. It depends on the Reynolds number based on the shear velocity and on a length associated with the size of the roughness, i.e., ($Re_* = U_* k_{ef}/\nu$), and it is often presented in the form (Perry et al 1969)

$$\frac{\langle U_k \rangle}{U_*} = \frac{1}{\kappa} \ln \frac{U_* k_{ef}}{\nu} + C. \tag{14}$$

The above equation is universal for a given roughness geometry in a pipe, channel and zero pressure gradient boundary-layer flow. The coefficient C is a constant whose value depends on the nature of the wall surface. For a hydraulically smooth flow ($k_{ef} U^*/\nu < 5$) $C = 5.5$ (see Yalin 1977). For a hydraulically rough flow and for a sufficiently large Reynolds number, the velocity distribution does not depend on viscosity and $U_k/U_* = B$ (const), so Eq. (13) becomes

$$\frac{\langle U(y) \rangle}{U_*} = \frac{1}{\kappa} \ln \frac{y}{k_{ef}} + B, \tag{15}$$

where y is the depth above the channel bottom. It is easy to see that the effective velocity origin is located above the theoretical bed at $y_0 = k_{ef} \exp(-\kappa B)$. It is worth emphasizing that Eq. 15 is identical with Nikuradse's log law for sand roughness. For sand roughness the universal constant $B = 8.5$ at $Re^* = k_e U_*/\nu > 70$ and $y_0 = k/30$.

This result needs some comments. Very precise measurements by Nezu and Rodi (1986) showed that our data for uniform flow, though formally valid only in the inner region, can be applied throughout the channel depth, with two universal constants: κ (von Karman's constant) and B. A close examination of velocity measurements showed a slight deviation from the logarithmic law in the region close to the water surface ($0.7 < y/h < 1$). To adjust Eq. (15) to the data, Coles' law was usually adopted (for details see Cordoso 1989, Nezu and Rodi 1986).

Sarkar and Dey (2010) showed that the double-averaged streamwise velocity above the interfacial sublayer follows the log law with an added constant of 5.57. A damping in the distributions of the double-averaged Reynolds shear stress within the form-induced and interfacial sublayers was observed. That damping is rather severe below the virtual bed level. The form-induced stress that is augmented mainly within the interfacial sublayer has a decelerating effect on the fluid.

Eq. (15) is widely used for a rough turbulent flow when the relative roughness is small $k_{ef}/h < 0.05$ (see Tu (1991). In the case of non-uniform flow over a rough bed, when the relative roughness is large, the coefficient B is no longer constant. Generally, the B value depends on the size, shape and distribution of roughness elements.

It is smaller than 8.5 in rough flows with a small relative roughness, e.g., Bayazit (1976) found that when $h/k_{ef} < 3$, B should be smaller than 8.5. It decreases as k_{ef}/h increases to 0.25, after which its value remains at approximately 5.0 for experiments with bed materials $D_s = 23.5$ mm (see Tu 1991).

Tu (1991) distinguished three zones for experiments with bed materials $D_s = 23.5$ mm:

1. zone 1 gives a constant B value of 8.5, when the roughness is relatively small, i.e., $D_s/h < 0.05$,
2. zone 2 shows a dependence of B on the relative roughness: B decreases as D_s/h increases to 0.25,
3. zone 3 suggests that B is independent of the relative roughness and approximately constant at 5.0 when $D_s/h > 0.25$.

How to determine the equivalent sand roughness, which is related to the grain diameter, is still a problem. Different investigators suggested different values. In Nikuradse tests in which uniform sands were used, $k_{ef} = D_s$; for non-uniform sands, Einstein and El-Sami assumed $k_{ef} = D_{65}$, Mayer-Peter chose $k_{ef} = D_{90}$, whereas Lane and Carlson, $k_{ef} = D_{75}$ (for more details, see Tu (1991).

As regards the location of the reference level, zero bed or theoretical bed (where $y = 0$), as it is called by different researches, Einstein and El-Sami found $y_0 = 0.20D$, for uniform roughness elements (hemispheres); Bayazit (1976), $y_0 = 0.35D$, also for hemispheres ($D = 23$ mm); and Grass (1991), $y_0 = 0.18D$, for rounded pebbles ($D = 9$ mm).

3.1. Measurements

Eq. (15) describes the velocity distribution for roughness type flow. However, the position of the virtual bed, the velocity origin (y_0) and the effective height of roughness elements k_{ef} should be determined depending on the situation. To calculate the typical k_{ef} and the position of the virtual bed for different geometries of roughness elements, the results of laboratory experiments were re-analyzed. These experiments are two Ph. D. dissertations by Mansour-Tehrani (University of London, 1992) and K. Koll (University of Karlsruhe 2002).

3.1.1. Mansour-Tehrani's Experiment (1992)

The experiment was carried out in a recirculating water channel 0.5 m wide, 6.2 m long and 0.3 m deep. The flow depth above the bed was kept at 50 mm for all experiments. Single layers of spherical roughness elements of different diameters (1.15 mm, 6 mm and 12 mm) were used to form rough beds along the first 2 m of the channel bed.

Laser Doppler anemometry was used to obtain velocity measurements in a fully developed turbulent flow over these rough beds. The measurements showed that

Table 1. Flow and bed roughness conditions of Mansour-Tehrani's (1992) measurements, y_0 = location of the velocity origin y_t = distance between the location of the velocity origin and the top of a roughness element (see Figure 1 for details)

Spherical elements	Roughness height = Diameter	Mean velocity	Shear velocity	Effective velocity origin	Location of velocity origin	Log law parameter	U_*k/ν
	$k = D$	U_m	U_*	y_0	y_t	B	Re_*
	mm	mm/s	mm/s	mm	mm	–	–
K1Q1	1.15	227.8	12.48	0.02	0.35	7.28	14.3
K1Q2	1.15	164.8	9.18	0.02	0.45	7.81	10.5
K1Q3	1.15	106.0	6.46	0.03	0.45	6.79	7.4
K6Q1	6	219.4	15.91	0.167	1.30	5.43	95.4
K6Q2	6	154.6	13.15	0.174	1.30	5.34	78.9
K6Q3	6	111.0	8.46	0.169	1.20	5.23	50.7
K12Q2	12	155.9	14.82	0.32	2.40	5.35	177.8
K12Q3	12	106.0	9.21	0.327	2.40	5.30	110.5

the flow becomes fully developed within the first meter of the channel, and that velocity profiles therefore remain unchanged. Thus, it can be assumed that a fully developed and steady channel flow was achieved in the test section.

The location of the origin y ($y = 0$) and the position of the velocity origin were determined by the Clauser method suggested by Perry at el (1969). This Clauser method is only valid when applied to the logarithmic region of the velocity profile, and therefore the determination of this region is very important. The velocity was measured at vertical positions directly above roughness elements and in between the elements above their tops. The lower limit of the log layer level was found to be about one third to one half of the roughness size. The position of the velocity origin, relative to the roughness crest height, is very sensitive to a specific roughness configuration. The position of velocity origins below the average roughness tops (y_t) and other hydraulic parameters are presented in Table 1 and Figure 1 (for details see Tehrani 1992).

It is possible to calculate the effective roughness height k_{ef} by adding two values: y_0 and the location of the velocity origin below the average roughness tops y_t. This sum indicates the location of the theoretical or virtual bed below the average roughness tops. It is easy to note from the table that k_{ef} grows with the size of roughness elements but never exceeds their size.

Summary of Mansour-Tehrani's measurements

For a non-dimensional parameter (U_*k/ν) in a range from ≈ 50 to ≈ 180, the velocity distribution does not depend on viscosity (rough turbulent flow) and the parameter B is constant, approximately equal to 5.3. For a much smaller shear

Reynolds number, $Re^* < 15$ (spherical roughness $k = 1.15$ mm), the parameter B increases up to 7.5, i.e., approaches Nikuradse's value for sand roughness.

3.1.2. Koll's Experiment (2002)

Velocity measurements were performed in a fully developed turbulent boundary layer formed on the rough bed of an open-channel water flow. The tests were performed in a tilting laboratory channel (0.3 m wide and 10 m long) for different bed roughness comprising artificial elements as well as natural riverbed material. Several bed roughness elements were used: 9 mm spherical elements glued to a bedplate (designated in Table 2 as RK-bill and RK-bs); 8 mm cubes glued to a bedplate with two different densities (cw and cd in Table 2); The series RK was performed with roughness elements of almost the same size but of different geometry (shape and density of the elements).

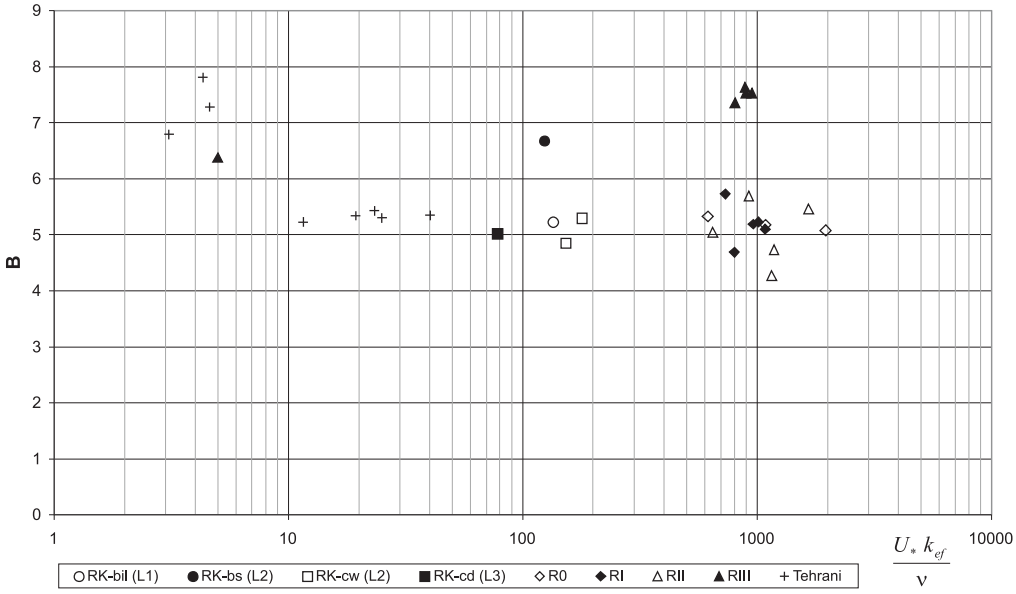

Fig. 2. Reconstruction of Nikuradse's graph for flows over spherical and cubical roughness elements and over river pebbles

Three beds comprised natural, river pebbles of 20 mm, 25 mm and 35 mm in average size (RI, RII and RIII, respectively in Table 2). The position of the virtual beds below the average roughness tops and other hydraulic parameters are presented in Table 2. The position of the theoretical (virtual) bed was calculated using a very precisely measured velocity and assuming the linear distribution of the mixing length in the roughness layer. Velocity distributions were measured at five places attached chosen gravels and then averaged. The roughness function

Table 2. Results of Koll's measurements (see Koll 2002); where: RK- bill - spherical roughness elements of 9 mm in diameter, arranged in line; RK-bs – spherical roughness elements of 9 mm in diameter, arranged in a stagger pattern; RK-cw (L2) – cubical roughness elements of 8 mm in size, sparsely arranged on the channel bed; RK-cw (L3) – the same as L2 with a slightly different relative submergence; RK-cd – cubical roughness elements of 8 mm in size, densely arranged; R0-RIII – Four beds comprising natural, river pebbles of 28 mm, 20 mm, 25 mm, 35 mm in average size and the rough density L/k = 2.1, 1.7, 3.2, 4, respectively; d – the zero-plane displacement, calculated from the linear regression between $u(z)$ and $\ln(z-d)$ (for details see Koll 2002); k_{ef} – height of the roughness interfering with the flow, equal to $(k-d)$; also measured from the top of roughness elements, i.e., $y_0 + y_t$ (see Figure 1); L – distance between neighboring roughness elements

	Rough. height	Mean velocity	Shear velocity	Zero-plane display-cement	Rough. effective height	Rough. density	Relative sub-mergence	Log law parameter	Re_*
	k	U_m	U_*	d	k_{ef}	L/k	h/k	$B = U_R/U_*$	$U_* k_{ef}/\nu$
	mm	mm/s	mm/s	mm	mm	–	–	–	–
RK-bill	8.3	551.3	56.6	5.9	2.4	1.9	13.11	5.23	135
RK-bs	8.3	558.0	56.7	6.1	2.2	1.85	13.17	6.68	124
RK-cwL2	8.0	534.3	57.5	5.8	3.2	4.0	14.04	4.85	153
RK-cwL3	8.0	542.9	56.5	4.8	3.2	4.0	20.34	5.30	179
RK-cd	8.0	567.4	56.2	6.6	1.4	1.9	20.12	5.02	78
R0-1	28	578.9	89.3	9.1	18.9	2.1	3.37	3.43	1726
R0-2	28	561.9	77.8	3.8	24.2	2.1	4.00	5.08	1963
R0-3	28	546.4	64.5	11.3	16.7	2.1	5.05	5.18	1086
R0-4	28	532.0	54.7	16.6	11.4	2.1	6.76	5.33	618
RI-1	20	455.2	53.5	5.5	14.5	1.7	4.87	4.69	800
RI-2	20	519.8	59.1	3.4	16.6	1.7	5.93	5.23	1014
RI-3	20	642.4	68.1	6.1	13.9	1.7	7.89	5.19	963
RI-4	20	742.3	76.1	10.4	9.6	1.7	9.83	5.73	732
RI-5	20	740.9	83.9	7.2	12.8	1.7	11.97	5.10	1084
RII-1	25	408.7	55.0	12.9	12.1	3.2	4.11	5.04	649
RII-2	25	483.7	60.8	9.7	15.3	3.2	5.02	5.69	923
RII-3	25	610.5	70.0	1.7	23.3	3.2	6.66	5.46	1661
RII-4	25	684.3	78.1	9.7	15.3	3.2	8.30	4.73	1183
RII-5	25	723.6	85.0	11.3	13.7	3.2	9.82	4.27	1156
RIII-1	35	407.1	54.7	19.4	15.6	4.0	2.90	7.63	889
RIII-2	35	451.2	60.8	18.9	16.1	4.0	3.59	7.53	895
RIII-3	35	595.5	69.8	23.1	11.9	4.0	4.73	7.36	806
RIII-4	35	664.3	77.8	23	12	4.0	5.88	7.53	951

(parameter B in Eq. (15)) was estimated directly from the definition as the ratio of velocity measured at the top of roughness elements (exactly at the upper boundary of the roughness layer) to the shear velocity.

Summary of Koll's measurements

- Spherical elements: the parameter B is greater for spherical elements arranged in a stagger pattern than for those arranged in a line. This can depend on the geometry of roughness elements forming the bed, but this conclusion is supported by only one case.
- Cubical elements: B value is greater for elements arranged sparsely than for those arranged densely. This is confirmed by only one case.
- For the non-dimensional parameter (Re_*) in the range $\approx 450 < (U_* k/\nu) \approx 1750$, the velocity distribution does not depend on viscosity, and the parameter B is in a range from 5 to 5.46. For the largest pebbles ($k = 35$ mm) and sparsely arranged gravel at $Re_* > 2000$, B is greater than 7.

3.2. Summary

Precise measurements of the flow velocity over spherical roughness elements of 6, 9 and 12 mm in diameter, cubes (8 mm) and gravel (20 mm and 25 mm) show that starting from a Reynolds number of $(U_* k_{ef}/\nu) = 75$, the flow condition can be described as a rough turbulent flow. For this type of flow, the velocity distribution does not depend on viscosity, and it is described by Eq. (15) with the effective roughness height k_{ef} and the parameter B taken from a range of 5 to 5.5. The coefficient k_{ef} is defined as the height of the roughness that interferes with the flow. In a pipe (Nikuradse case) and in an open channel with a flat sand bed, k_{ef} is equal to the diameter of the sand grains and the parameter B takes a value of 8.5.

4. Flows in Gravel-bed Channels in the Presence of a Pressure Gradient

For environmental engineers, the knowledge of the vertical distribution of the mean velocity in open-channel flows is particularly important, especially for non-uniform flows, which are more natural in rivers or open-channel flows. However, efforts to assess this velocity distribution have concentrated mainly on uniform flow conditions. Thus, the non-uniform flow is of interest here. First, the basic equation of a two-dimensional vertical velocity profile is developed for flows with a pressure gradient.

Non-uniform flows are produced by changes in the channel geometry as one uniform-flow condition changes to another and in accelerating and decelerating flows. Depending on the sign of the pressure gradient, one can distinguish families of velocity profile results which correspond to the following conditions:

- $d < P > /dx < 0$ accelerating flow,
- $d < P > /dx = 0$ zero-pressure gradient flow this case was already discussed in Chapter 3,
- $d < P > /dx > 0$ decelerating flow,

where P stands for free stream pressure. Some authors have studied the effect of dP/dx on velocity distributions. Most of them dealt with decelerating flows. The formulation of the velocity distribution in equilibrium turbulent boundary layers concern for decelerating flows, as it was reviewed by Yaglom (1979). He showed that in the overlapping region the velocity distribution follows the logarithmic law, which holds for accelerating flows as long as they are in a local equilibrium. However, it can be expected that the logarithmic law will probably not hold up to arbitrarily high values of the pressure gradient. In the case of accelerating flows, the criterion for the breakdown of the universal law of the wall is given by equation (see Cordoso 1989)

$$\Delta p = \frac{\nu}{\rho U_*^3} \frac{dP}{dx} < -0.02. \tag{16}$$

Generally, the effect of spatial acceleration on the deformation of the mean velocity field, can be written on the basis of some measurements (see Cordoso 1989, Tu and Yang 2009) that

- The velocity distributions could no longer be represented entirely by the universal log law. Deviations from this law are to be attributed mainly to acceleration. The existence of an inner layer, which is in equilibrium and follows the law of the wall, and of an outer layer, which deviates from that law, can be postulated. The inner log law seems to extend up to about 0.05 of the flow depth.
- Bagherimiyab and Lemmin (2010) found in their experiments that during accelerating and decelerating flows, all mean velocity profiles followed a logarithmic law in the inner layer. However, differences in the profile form were observed, i.e., the accelerating flow profile has a greater shear velocity than the decelerating one.
- The mixing length distribution is self-similar up to $y = 0.05h$, where it also follows Prantdl's mixing length hypothesis. The log law can also be used for unsteady flow.
- For the equal water depth, the point velocity in the rising branch (for accelerating flow) is generally greater than the one in the falling branch (for decelerating flow).
- For the equal vertical-averaged velocity, the velocity profiles fall on one another, except near the water surface, where the point velocities in the rising branch are usually greater than the ones in the falling branch.
- For a given hydrograph, the friction velocity in accelerating flow (rising branch) is usually higher that the one in decelerating flow (falling branch).
- The vertical shear-stress distributions for the rising branch are usually concave, implying accelerating flow (when dp/dx is negative); those for the falling branch are convex, implying decelerating flow (when dp/dx is positive). If the longitudinal pressure gradient is zero, the constant shear stress layer is to be observed.

– At the same water height, the shear stress in accelerating flow is larger that the one in decelerating flow.
– Turbulence intensity decreases for negative pressure gradients flows and increases for positive pressure gradient flows.

4.1. Basic Equations

If the flow depth varies with respect to the distance, the flow is called gradually varied. Equations describing the gradually varied flow, in accelerating and decelerating flows, are derived under the following simplifying assumptions:

1. The slope of the channel bottom is small.
2. The pressure distribution at a channel section is hydrostatic.
3. The head losses in a gradually varied flow may be determined by using an equation for head losses in uniform flows, i.e., $U_*^2 = ghS_f$.

It is very natural to assume that for wide open-channel flow all terms in the lateral, z-momentum equation are zero, and it is easy to show from Eq. (8) that the y-momentum equation for steady flow takes the form

$$\begin{aligned} \langle U\rangle \frac{\partial \langle V\rangle}{\partial x} + \langle V\rangle \frac{\partial \langle V\rangle}{\partial y} = \\ = g_y - \frac{1}{\rho}\frac{\partial \langle P\rangle}{\partial y} - \frac{\partial \langle \overline{uv}\rangle}{\partial x} - \frac{\partial \left\langle \overline{v^2}\right\rangle}{\partial y} - \frac{\partial \langle \widetilde{uv}\rangle}{\partial x} - \frac{\partial \left\langle \widetilde{v^2}\right\rangle}{\partial y} + \\ + \frac{\partial}{\partial x}\left\langle \nu \frac{\partial V}{\partial x}\right\rangle + \frac{\partial}{\partial y}\left\langle \nu \frac{\partial V}{\partial y}\right\rangle, \end{aligned} \tag{17}$$

where $g_y = g\cos\theta$. We will need the following assumptions:

1. flow is unidirectional with the double-averaged velocity vector equal to ($< U > + u, v$);
2. two x-derivatives of turbulent and form stresses can be neglected.

Under the above assumptions, the y-momentum equation is simplified to

$$0 = g_y - \frac{1}{\rho}\frac{\partial \langle P\rangle}{\partial y} - \frac{\partial \left\langle \overline{v^2}\right\rangle}{\partial y} - \frac{\partial \left\langle \widetilde{v^2}\right\rangle}{\partial y}. \tag{18}$$

After integrating Eq. (18) in the domain $[y, h]$, one can get

$$\langle P\rangle(y) = \rho g h\cos\theta\left(1 - \frac{y}{h}\right) + \left(\left\langle \overline{v^2}\right\rangle(h) - \left\langle \overline{v^2}\right\rangle(y)\right) + \left(\left\langle \widetilde{v^2}\right\rangle(h) - \left\langle \widetilde{v^2}\right\rangle(y)\right). \tag{19}$$

One can conclude from Eq. (19), that the pressure distribution is hydrostatic only for a small bed slope, vertically homogeneous turbulence and the spatial deviation of vertical velocity equal to zero.

The x-momentum equation under similar assumptions as those for the y-equation Eq. (17), takes the form

$$\langle U\rangle \frac{\partial \langle U\rangle}{\partial x} = g_x - \frac{1}{\rho}\frac{\partial \langle P\rangle}{\partial x} - \frac{\partial \langle \overline{uv}\rangle}{\partial y} - \frac{\partial \left\langle \overline{u^2}\right\rangle}{\partial x} - \frac{\partial \langle \widetilde{uv}\rangle}{\partial y} - \frac{\partial \left\langle \widetilde{u}^2\right\rangle}{\partial x} + \nu\frac{\partial^2 \langle U\rangle}{\partial y^2}, \quad (20)$$

where $g_x = g\sin\theta$.

We can certainly assume that two terms related to the x-derivative of Eq. (20), i.e., the longitudinal component of the turbulent velocity squared and the deviation velocity squared, are negligibly small and can be omitted in further consideration. It is obvious, from Eq. (20), the total shear stresses at the bed as the sum of viscous, turbulent and form-induced stresses in the form

$$\frac{\tau_b}{\rho h} = \frac{\partial \langle \overline{uv}\rangle}{\partial y} - \frac{\partial \langle \widetilde{uv}\rangle}{\partial y} + \nu\frac{\partial^2 \langle U\rangle}{\partial y^2}. \quad (21)$$

For a small bed slope, $\sin\theta \sim \tan\theta = S_0$ and hydrostatic pressure $P = \rho g h$, and Eq. (20) can be re-written in the form

$$\langle U\rangle \frac{\partial \langle U\rangle}{\partial x} + \frac{1}{\rho}\frac{\partial \langle P\rangle}{\partial x} = g_x S_0 - \frac{\tau_b}{\rho h} = g\,(S_0 - S_f). \quad (22)$$

To define the derivative dU/dx in Eq. (22), one can use the continuity equation

$$h\frac{\partial \langle U\rangle}{\partial x} + \langle U\rangle \frac{\partial h}{\partial x} = 0 \rightarrow \frac{\partial \langle U\rangle}{\partial x} = -\frac{1}{h}\langle U\rangle \frac{\partial h}{\partial x}. \quad (23)$$

Taking into account the above two equations (Eqs. (22)–(23) and applying the formula for the bed shear $\tau_b/\rho = U_*^2 = ghS_f$, we may, after some algebra, write a formula for the friction velocity:

$$U_{*P} = \sqrt{gh\left[S_0 - \frac{dh}{dx}(1 - Fr^2)\right]} \quad \text{where} \quad Fr = \frac{\langle U\rangle}{\sqrt{gh}}. \quad (24)$$

The above equation can only be used for steady non-uniform flows. It is also valid in unsteady flows if the wave is a kinematic one, but it cannot be extended to unsteady flows if the wave is dynamic. We are now in a position to show the possibility of applying the MLH to describe velocity profiles. We can certainly assume that the total shear stress can be modeled by a formula similar to the MLH as shown in Eq. (12).

$$-\langle\overline{uv}\rangle(y) = U_{*P}^2\left(1-\frac{y}{h}\right). \tag{25}$$

Solving Eq. (25) for a small $y << h$ and assuming the legitimacy of Prandtl's MLH with $l = \kappa y$ (see Eq. (12)), one obtains the log law in the form

$$\frac{\langle U\rangle(y)}{U_{*P}} = \frac{1}{\kappa}\ln\frac{y}{k_{ef}} + \frac{\langle U\rangle(k_{ef})}{U_{*P}}, \tag{26}$$

where U_{*P} is defined by Eq. 24, κ is von Karman's constant, k_{ef} is the effective roughness height, $< U > (k_{ef})$ is the value of $< U >$ at k_{ef}, and the last term of the above equation can be recognized as the additive constant and designated as B_P.

To define the additive constant in the case of non-uniform flow over a gravel bed, the measuring data of Afzalimehr and Anctil (2000) were analyzed.

4.2. Measurements by Afzalimehr and Anctil (2000)

The behavior of the velocity distributions along a gravel-bed channel (8.8 m long and 0.6 m wide) is investigated experimentally in the presence of a negative pressure gradient (accelerating flow) in channel flows at different water depths ranging from 0.2 m to 0.3 m. In order to obtain an accelerating flow in which the flow depth decreases along the flow direction, a tailgate was installed downstream. To ascertain that the flow was fully developed, velocity distributions were measured at three sections, 1.9, 2.4 and 2.9 m, so as to check the similarity of these profiles. The bed was covered with gravel material ranging in size from 16.8 mm to 34 mm with a standard deviation of 3.9 mm and a median value of 25.4 mm.

Vertical velocity profiles were measured for three different flow discharges (Q = 0.04; 0.06; 0.08 m^3/s), and four different bottom slopes. The range of relative submergence for all measured velocity profiles was $7.5 < h/d < 13$, and the range of the aspect ratio was $1.82 < w/h < 3.16$, where w is the channel width.

The mean velocity measurements were performed with a downlooking Acoustic Doppler Velocimeter. A detailed analysis of all velocity profiles confirmed that the logarithmic law is valid for gravel-bed channels as long as it is applied to the inner layer of the flow ($y/h < 0.2$). On the basis of these velocity profiles, the shear velocity was estimated from the parameter of regression of the velocity and $\ln y$ (for more details see Clauser 1956).

The numerical constant of integration B_P was calculated on the basis of the measured velocity, estimated friction velocity, D_{50}, and von Karman's constant. The reference level was $0.2d_{50}$ below the top of the plane passing through the average tops of the gravel. Results are displayed in Figure 3, and they show that the parameter B_P increases with the pressure gradient (dh/dx). The data is insufficient to establish any formula for the relation between B_P and dh/dx, but the tendency is quite clear.

Table 3. Measured and calculated parameters: d_{50} = median value of grain sizes, h = water depth, U_m = cross-section average velocity, U_* = friction velocity, S_0 = bed slope, B_P = additive constant in the log law, $Re_* = U_{*P} * d_{50}/\nu$

Run	d_{50}	H	U_m	$U_{*Clauser}$	B_P	S_0	$-$ grad h	Re_*
1	0.0254	0.253	0.264	0.026	6.907	0.007	0.00758	660.4
2	0.0254	0.286	0.233	0.024	6.155	0.007	0.00742	609.6
3	0.0254	0.253	0.395	0.036	7.725	0.007	0.00792	914.4
4	0.0254	0.330	0.404	0.037	7.008	0.007	0.00809	939.8
5	0.0254	0.270	0.247	0.024	6.882	0.010	0.01045	609.6
6	0.0254	0.284	0.352	0.030	8.197	0.010	0.01069	762.0
7	0.0254	0.261	0.511	0.043	8.559	0.010	0.01170	1092.2
8	0.0254	0.255	0.367	0.036	6.928	0.007	0.00780	914.4
9	0.0254	0.190	0.351	0.032	8.438	0.015	0.01700	812.8
10	0.0254	0.253	0.527	0.040	9.928	0.015	0.01780	1016.0
11	0.0254	0.253	0.264	0.021	9.324	0.020	0.02076	533.4
12	0.0254	0.253	0.395	0.030	9.920	0.020	0.02170	762.0
13	0.0254	0.253	0.527	0.040	9.928	0.020	0.02300	1016.0

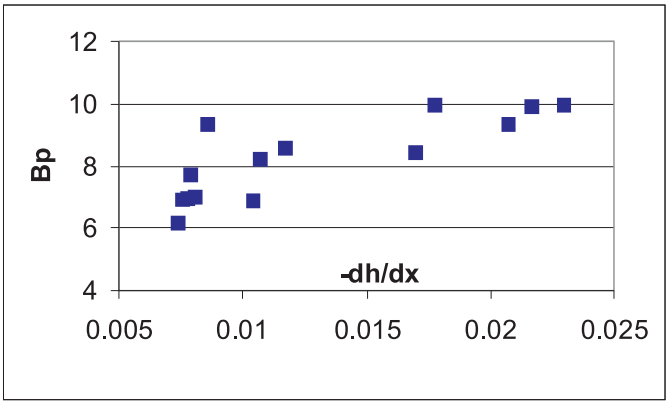

Fig. 3. Relation between B_P and the pressure gradient in the presence of a negative pressure gradient based on measurements by Afzalimehr and Anctil (2000)

The relation between B_p and the Reynolds number is shown in Figure 4. One can see that the coefficient B_P ranges from 6 to 10 as Re_* ranges from 500 to 1100 (see Fig. 4). These calculations are based on the measured velocities in the inner region of the boundary layer, as well as von Karman's constant and the reference level (location of the theoretical bed $y = 0$ plane).

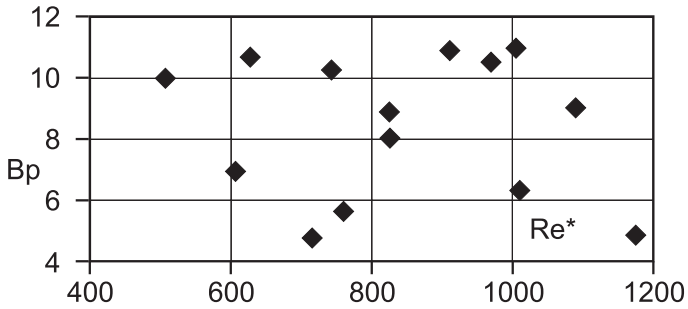

Fig. 4. Relation between B_p and the Reynolds number Re_* based on measurements by Afzalimehr and Anctil (2000)

5. Conclusion

- The logarithmic velocity profile appears in any stationary, unidirectional flows, as well as in accelerating flows in a gravel bed channel, but the friction velocity should be re-defined according to Eq. (24). The same applies to decelerating flows with a positive pressure gradient, but only if the gravitational force exceeds the pressure gradient.
- The B_P coefficient for accelerating flows depends on the pressure gradient and grows with the growing gradient h (see Fig. 3).
- The B_P coefficient for rough turbulent flows is almost independent of the Reynolds number (see Fig. 4). The result is similar to Nikuradse's graph defined for a flat, sand bed, i.e. the velocity distribution does not depend on viscosity but on the size and nature of the roughness.

Acknowledgments

This work was supported by grant N N306 658140 from The National Science Centre Grant, Poland. The author is grateful to Dr. K. Koll and to professor D. Knight for excellent data, as well as for useful discussions and suggestions. He also wishes to express his thanks to Dr P. Rowinski for reviewing an early draft of the results and for his helpful criticism.

References

Aberle J. (2007) Measurements of armour layer roughness geometry function and porosity, *Acta Geophysica*, 55, 23–32. DOI: 10.2478/s11600-006-0036-5.

Aberle J., K. Koll, A. Dittrich (2008) Form induced stresses over rough gravel-beds, *Acta Geophysica*, 56 **(3)**, 584–600. DOI: 10.2478/s11600-008-0018-x.

Afzalimehr H. & Anctil F. (2000) Accelerating shear velocity in gravel-bed channels, *Hydrological Sciences-Journal*, 45 **(1)**, 113–124.

Bayazit M. (1976) Free Surface Flow in a Channel of Large Relative Roughness, *J. Hydr. Res.*, 14 **(2)**, 115–126.

Gimenez-Curto L. A. & Corniero Lera M. A. C. (1996) Oscillating turbulent flow over rough surfaces, *Journal of Geophysical Research*, 101 **(C9)**, 20745–20,758.

Guo J., Julien P. Y., Meroney R. N. (2005) Modified log-wake law for zero-pressure-gradient turbulent boundary layers, *Journal of Hydraulic Research*, **43**, (4), 421–430.

Kamphuis J. W. (1974) Determination of Sand Roughness for Fixed Beds, *J. Hydr. Res.*, 12 **(2)**, 193–203.

Kirkgoz S. M. (1989) Turbulent velocity profiles for smooth and rough open channel flow, *J. Hydr. Engrg.*, 115 **(11)**, 1543–1561.

Koll K. (2002) *Transport of Sediment and Velocity Distribution in Rough Channels*, Ph.D. Dissertation, University of Karlsruhe (in German).

Mansour-Tehrani M. (1992) *Spatial Distribution and Scaling of Bursting Events in Boundary Layer Turbulence over Smooth and Rough Surfaces*, Ph.D. Dissertation, University of London.

McLean S., Dittrich A., Aberle J. (2002) Zero-plane displacement for rough-bed open-channel flows, *Proceedings of The International Conference on Fluvial Hydraulics River Flow 2002*, Sep. 4–6, Louvain-la-Neuve, Belgium, 83–92.

Nikora V., Goring D., McEven I., Griffiths G. (2001) Spatially averaged open-channel flow over rough bed, *J. Hydrual. Eng.*, 127 **(2)**, 123–133.

Nikora V., Koll K., McEwan I., McLean S., Dittrich A. (2004) Spatial Averaging Concept for Rough-bed Open-Channel and Overland Flows, *Advances in Hydro-Sciences and -Engineering*, Vol. VI, ICHE Conferences, Brisbane.

Nikora V., McEwan I., McLean S., Coleman S., Pokrajac D., Walters R. (2007) Double averaging concept for rough-bed open-channel and overland flows: Theoretical background, *J. Hydraulic Eng.*, 133 **(8)**, 873–883.

Perry A. E., Schofield W. H., Joubert P. N. (1969) Rough Wall Turbulent Boundary Layers, *J. Fluid Mech.*, 37, 383–413.

Sarkar S., Day S. (2010) Double-averaging turbulence characteristics in flow over a gravel bed, *Journal of Hydraulic Research*, 48 **(6)**, 801–809.

Slattery J. C. (1999) *Advanced Transport Phenomena*, Cambridge University Press, Cambridge.

Yaglom A. M. (1979) Similarity laws for constant-pressure and pressure-gradient turbulent wall flows, *Ann. Rev. Fluid Mech.*, 11, 505–540.

Yalin M. S. (1977) *Mechanics of Sediment Transport*, Pergamon Press, Oxford.

Yang S-Q. (2009) Veloicty distribution and wake-law in gradually decelerating flows, *Journal of Hydraulic Research*, 47 **(2)**, 177–184.

Appendix. Some definitions

1. *Outer layer*. In this region, viscous effects are negligible, and spatially-averaged equations are identical to time-averaged equations. This layer, including the near-surface and wake regions (Nezu and Nakagawa 1993), is similar to the outer layer for open-channel flows over hydraulically smooth beds.
2. *Logarithmic layer*. In this intermediate flow region, viscous effects are negligible, and spatially-averaged equations are identical to time-averaged equations, as for the outer layer. This layer is similar to the logarithmic layer for flows with hydraulically smooth beds.

3. *Dispersive sublayer*. Flow in this region is influenced by individual roughness elements, and the dispersive sublayer occupies the region just above roughness crests.
4. *Interfacial sublayer*. This sublayer is also influenced by individual roughness elements and occupies the flow region between roughness crests and troughs (i.e., where the roughness geometry function $\phi(y)$ changes from 1 to 0).

The dispersive and interfacial sublayers together can be identified as the roughness layer. Similar to boundary layers with hydraulically smooth beds, we can identify the flow region occupied by the logarithmic and roughness layers as the wall or inner layer. The same analogy suggests that the role of the roughness layer for hydraulically rough beds is similar to that of the viscous and buffer sublayers for smooth beds. The interfacial sublayer could be interpreted similarly to the viscous sublayer, while the dispersive sublayer, as the buffer sublayer. At the boundary between the logarithmic layer and the roughness layer, the shear stress and turbulence intensities should attain maximum values as in smooth-wall flows.